Frontiers in Heat and Mass Transfer

Tech Science Press

DOI: 10.32604/fhmt.2024.052223

ARTICLE

# Exergy Analysis of a Solar Vapor Compression Refrigeration System Using R1234ze(E) as an Environmentally Friendly Replacement of R134a

**Zakaria Triki[1], Ahmed Selloum[1], Younes Chiba[1], Hichem Tahraoui[1,2], Dorsaf Mansour[3], Abdeltif Amrane[4,*], Meriem Zamouche[5], Mohammed Kebir[6] and Jie Zhang[7]**

[1]Laboratory of Biomaterials and Transport Phenomena, University of Medea, Medea, 26000, Algeria

[2]Laboratoire de Génie des Procédés Chimiques, Department of Process Engineering, University of Ferhat Abbas, Setif, 19000, Algeria

[3]Chemistry Department, College of Sciences, University of Hail, Hail, 55223, Saudi Arabia

[4]Univ Rennes, Ecole Nationale Supérieure de Chimie de Rennes, CNRS, ISCR–UMR6226, Rennes, F-35000, France

[5]Laboratoire de Recherche sur le Médicament et le Développement Durable (ReMeDD), Faculty of Process Engineering, University of Salah Boubnider Constantine 3, Constantine, 25000, Algeria

[6]Research Unit on Analysis and Technological Development in Environment (UR-ADTE/CRAPC), Bou-Ismail, Tipaza, 42004, Algeria

[7]School of Engineering, Merz Court, Newcastle University, Newcastle upon Tyne, NE1 7RU, UK

*Corresponding Author: Abdeltif Amrane. Email: abdeltif.amrane@univ-rennes1.fr

Received: 27 March 2024 Accepted: 13 June 2024 Published: 30 August 2024

## ABSTRACT

Refrigeration plays a significant role across various aspects of human life and consumes substantial amounts of electrical energy. The rapid advancement of green cooling technology presents numerous solar-powered refrigeration systems as viable alternatives to traditional refrigeration equipment. Exergy analysis is a key in identifying actual thermodynamic losses and improving the environmental and economic efficiency of refrigeration systems. In this study exergy analyze has been conducted for a solar-powered vapor compression refrigeration (SP-VCR) system in the region of Ghardaïa (Southern Algeria) utilizing R1234ze(E) fluid as an eco-friendly substitute for R134a refrigerant. A MATLAB-based numerical model was developed to evaluate losses in different system components and the exergy efficiency of the SP-VCR system. Furthermore, a parametric study was carried-out to analyze the impact of various operating conditions on the system's exergy destruction and efficiency. The obtained results revealed that, for both refrigerants, the compressor exhibited the highest exergy destruction, followed by the condenser, expansion valve, and evaporator. However, the system using R1234ze(E) demonstrated lower irreversibility compared to that using R134a refrigerant. The improvements made with R1234ze are 71.95% for the compressor, 39.13% for the condenser, 15.38% for the expansion valve, 5% for the evaporator, and 54.76% for the overall system, which confirm the potential of R1234ze(E) as a promising alternative to R134a for cooling applications.

## KEYWORDS

Solar cooling; vapor compression refrigeration; eco-friendly refrigerant; thermodynamic losses; exergy analysis

**Nomenclature**

| | |
|---|---|
| $A$ | Surface area of the module ($m^2$) |
| $\dot{E}x$ | Exergy in any state (W) |
| $\dot{E}x_{in}$ | Input exergy (W) |
| $\dot{E}x_{out}$ | Output exergy (W) |
| $\dot{E}x_{loss}$ | Exergy loss (W) |
| $\dot{E}x_{D}$ | Rate of exergy destruction (W) |
| $\dot{E}x_{electrical}$ | Electrical exergy (W) |
| $\dot{E}x_{thermal}$ | Thermal exergy (W) |
| $FF$ | Fill factor |
| $G$ | Global irradiance ($W/m^2$) |
| $h$ | Enthalpy (kJ/kg) |
| $h_{conv}$ | Convective heat transfer coefficient ($W/m^2.K$) |
| $h_{rad}$ | Radiative heat transfer coefficient ($W/m^2.K$) |
| $I$ | Current (A) |
| $I_{mp}$ | Current at maximum power point (A) |
| $I_{sc}$ | Short-circuit current (A) |
| $\dot{m}_r$ | Mass flow rate of refrigerant (kg/s) |
| $NOCT$ | Nominal operating cell temperature (°C) |
| $\dot{Q}$ | Heat emitted to the surrounding (W) |
| $\dot{Q}_e$ | Net refrigeration effect produced (W) |
| $s$ | Entropy (kJ/kg.K) |
| $T$ | Temperature (K) (°C) |
| $T_b$ | Constant boundary temperature (room temperature) (K) |
| $T_s$ | Temperature at the surface of the Sun (K) |
| $T_{sky}$ | Sky temperature (K) |
| $U$ | Overall heat loss coefficient ($W/m^2.K$) |
| $V$ | Voltage (V) |
| $V_{mp}$ | Voltage at maximum power point (V) |
| $V_{oc}$ | Open-circuit voltage (V) |
| $V_w$ | Wind velocity (m/s) |
| $\dot{W}_{comp}$ | Work of the compressor (W) |

**Greek Symbols**

| | |
|---|---|
| $\varepsilon$ | Emissivity of the module |
| $\eta_{ex}$ | Exergetic efficiency |
| $\sigma$ | Boltzmann constant ($W/m^2.K^4$) |

**Subscripts**

| | |
|---|---|
| 0 | Dead state |
| $a$ | Ambient |
| $comp$ | Compressor |
| $cond$ | Condenser |
| $evap$ | Evaporator |
| $exp$ | Expansion valve |
| $m$ | Module |

**Abbreviations**

| | |
|---|---|
| *COP* | Coefficient of performance |
| *HFC* | Hydro-Fluoro-Carbon |
| *HFO* | Hydro-Fluoro-Olefin |
| *GWP* | Global Warming Potential |
| *ODP* | Ozone Depletion Potential |
| *SP-VCR* | Solar-powered vapor compression refrigeration |
| *PV* | Photovoltaic |
| *VCR* | Vapor compression refrigeration |

## 1 Introduction

Refrigeration technologies play a pivotal role in modern society, impacting various aspects of daily life, industry, and the economy. It enables the preservation and storage of perishable goods, extending their shelf life and ensuring food safety. Moreover, refrigeration is indispensable in numerous industries, including pharmaceuticals, healthcare, and manufacturing, where precise temperature control is critical for preserving the efficacy and quality of products and materials. Beyond its commercial applications, refrigeration technology contributes to improving living standards and comfort, as evidenced by its widespread use in air conditioning and climate control systems. In addition to enhancing comfort and productivity, efficient refrigeration technologies also play a crucial role in energy conservation and environmental sustainability. By employing advanced refrigeration systems with high energy efficiency and low environmental impact, society can reduce energy consumption, lower greenhouse gas emissions, and mitigate climate change [1,2].

In recent years considerable attention has been paid to global warming due to the greenhouse effect. The integration of low global warming potential (GWP) refrigerants into vapor compression refrigeration (VCR) systems marks a significant advancement in environmental sustainability and climate mitigation efforts. These refrigerants, characterized by their reduced impact on global warming compared to traditional high GWP alternatives, offer a compelling solution for reducing greenhouse gas emissions in cooling applications. In this context, Hydro-Fluoro-Olefin (HFO) refrigerants like R1234yf and R1234ze(E) have emerged as promising alternatives and potential substitutes for Hydro-Fluoro-Carbon (HFC) refrigerants due to their low GWP values [3].

Solar-powered vapor compression refrigeration (SP-VCR) systems represent a pioneering approach to sustainable cooling solutions. By harnessing solar power through photovoltaic (PV) or solar thermal technologies, these innovative systems offer a renewable and environmentally friendly alternative to conventional refrigeration methods. This approach not only reduces reliance on fossil fuels and grid electricity but also mitigates greenhouse gas emissions, contributing to climate change mitigation efforts. Moreover, SP-VCR systems have significant potential for applications in off-grid and remote areas, where access to electricity is limited or unreliable, offering sustainable solutions for a more resilient and energy-efficient future [4].

Exergy analysis of SP-VCR systems holds significant importance in assessing their performance, efficiency, and overall sustainability. Unlike traditional energy analysis, which focuses solely on energy quantity, exergy analysis considers the quality of energy and its potential to perform useful work. In addition, performing an exergy analysis enables a more detailed identification of inefficiencies and system losses, facilitating improved system design and pinpointing opportunities for optimization.

Furthermore, exergy analysis enables the comparison of different system configurations and refrigerants, helping to identify the most efficient and environmentally friendly options. The principles and methodologies of exergy analysis are well-established in the literature [5,6].

Several theoretical and experimental studies have investigated the exergy efficiency of SP-VCR systems. Some other researchers have compared the exergy analysis of VCR systems powered by conventional electricity and those powered by electrical energy from PV solar panels. Sudhakar et al. [7] conducted a study on a 36 W PV solar module, evaluating its thermal, electrical, and exergy production. Using experimental data, they determined the energy and exergy efficiencies of the module, finding energy efficiency ranging from 6% to 9% throughout the day, while exergy efficiency varied between 8% and 10%. Their analysis highlighted the significant impact of PV module temperature on exergy efficiency, suggesting that efficient heat dissipation from the module's surface could enhance exergy efficiency by mitigating exergy losses associated with increased temperature.

Jemaa et al. [8] performed an energy and exergy analysis to assess the viability of R1234ze(E) as a substitute for R134a in vapor compression chillers. The obtained results revealed that no significant disparities are noted in the energy and exergy efficiencies for both refrigerants. However, the irreversibility detected in the unit utilizing R1234ze(E) is less than that observed with the R134a refrigerant.

A comparative study by Dhondge et al. [9] investigated the energy and exergy performances of a refrigerator powered by photovoltaic solar energy for vaccine storage, comparing refrigerants R-134a and nano-refrigerant (R-134a + 0.5% $Al_2O_3$). Their analysis focused on exergy destruction, exergy efficiency, and coefficient of performance (COP). They observed minimal exergy losses at higher evaporation temperatures, with the majority occurring in the evaporator and compressor, accounting for 36% to 37% of total system losses.

Hayan et al. [10] established a micro-refrigeration experimental system powered by photovoltaic generation, operating with R134a refrigerant. They investigated changes in cooling capacity, load power, and system efficiency under varying weather conditions. Their findings suggested that the appended battery improved system stability, with the weather having negligible effects on indoor refrigeration system operation. Exergy analysis revealed compression process exergy loss as the largest contributor, comprising over 80% of total system losses, with refrigeration system exergy efficiency reaching around 28% under all weather conditions.

Omer et al. [11] conducted an experimental analysis of a small DC refrigerator driven by a solar photovoltaic panel in Baghdad. Their study, conducted with a 5-liter water load refrigerator, identified an average optimal exergy loss value of 24.63% at an evaporating temperature of –6°C. In a recent study, Amaris et al. [12] evaluated the energy and exergy performance of a 200 W direct-current solar PV refrigerator with internal heat exchange, using R600a, R290, R717, and R134a as base cases for autonomous solar refrigeration. Their findings suggested that while the internal heat exchanger reduced exergy destruction in the compressor and expansion valve, it increased in the condenser for R134a, R600a, and R290.

Khan et al. [13] investigated the performance of two novel compression absorption cascade refrigeration systems, the ejector compression absorption cycle and ejector injection compression absorption cycle, in comparison to traditional systems. Their analysis revealed that while the COP of all layouts augments linearly with increasing evaporator temperature, the exergy efficiency decreases at different rates, making the cascade systems more efficient for low-temperature applications.

In another study, Nabil et al. [14] conducted a comprehensive thermo-economic analysis and Python simulation model evaluation of a novel advanced three-stage cascade refrigeration (ATCR) system in terms of exergy, energy, and economics. The results of their research indicated the superior performance of the proposed refrigeration system in comparison to conventional triple cascade refrigeration systems (TCR), thereby demonstrating improved cascade refrigeration efficiency. In addition, the ATCR system achieved a notable 19.33% reduction in compressor work input, resulting in a 22% increase in the COP compared to the conventional VCR-based TCR.

Recently, Albà et al. [15] conducted a holistic 4E (Energy, Exergy, Economic, Environmental) analysis on low GWP refrigerants, integrating statistical methods with advanced equations of state to evaluate the effect of design factors on the energy and exergy performance of air-conditioning cooling cycles. The results demonstrated the potentiality of R1234ze(E) and R1225ye(Z) in terms of environmental, safety, and technical criteria in basic cooling cycles under specific operating conditions, highlighting their appropriateness for low-medium temperature applications.

Also, Al-Rbaihat et al. [16] presented a detailed analysis of energy and exergy on a single-effect solar ammonia–water ($NH_3$–$H_2O$) absorption refrigeration cycle (ARC) using TRNSYS and EES software. The results showed that the generator is the main source of exergy destruction in all operating conditions, highlighting its crucial role in ARC, while the exergy destruction from the precooler, pump, and expansion valves was negligible in comparison.

Despite the extensive body of literature on the subject, there appears to be a notable absence of comprehensive exergy analyses for SP-VCR systems using R1234ze(E) fluid as an alternative to R134 refrigerant for cooling purposes. This study seeks to fill the identified gaps in existing research. Moreover, the utilization of PV solar energy to power refrigeration systems represents a burgeoning area of exploration and innovation, particularly in regions abundant in sunlight and isolated areas lacking access to the electrical grid.

The main purpose of this paper is to assess the exergy performance of a SP-VCR system in the Ghardaïa region of southern Algeria. Two working fluids have been investigated and compared: HFC high-GWP refrigerant, R134a, and HFO low-GWP refrigerant, R1234ze(E), recently introduced as a more environmentally friendly alternative.

Despite existing studies in related areas, there is a notable absence of detailed exergy analyses specifically targeting this combination of solar energy and refrigeration technology and highlighting its advantages over traditional refrigerants. By addressing this gap, the study contributes to the emerging field of utilizing PV solar energy for refrigeration, particularly in regions with abundant sunlight, and isolated sites not connected to the electricity network.

In addition, this research provides the scientific community with valuable insights into optimizing refrigeration system performance and reducing environmental impact by adopting eco-friendly refrigerants. Potential prospects of the proposed research include enhanced energy efficiency, reduced operational costs, and improved regulatory compliance for industrial refrigeration applications. By fostering sustainable development in refrigeration technology, this study supports the transition to greener alternatives and contributes to the broader goal of environmental sustainability.

## 2 Materials and Methods

### *2.1 System Description*

Fig. 1 illustrates the main elements of the SP-VCR system under study. At the core of this system are PV panels, which capture sunlight and convert it into electricity through the photovoltaic effect.

As sunlight strikes the solar cells, they generate DC electricity, which is then converted into AC by an inverter, making it suitable for powering the components of the refrigeration system. The controller manages energy flow by regulating solar energy input, optimizing battery charging and discharging, and maintaining system performance through temperature and load management. It also monitors system status, detects faults, and provides user interface functionalities.

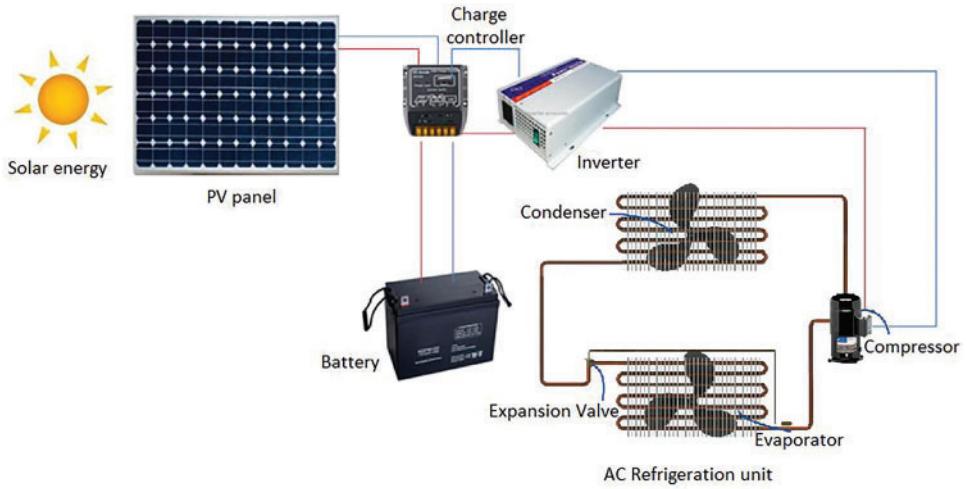


(a)

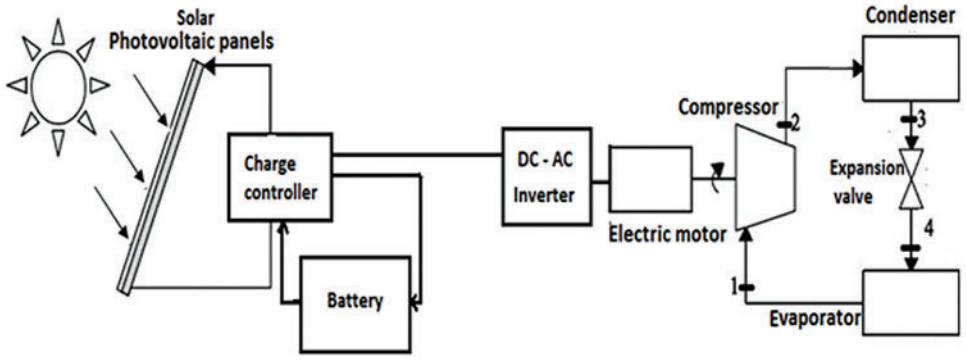


(b)

**Figure 1:** Pictorial and schematic diagrams of the solar-powered vapor compression refrigeration system

The battery stores excess solar energy for use during low solar radiation periods or at night, ensuring uninterrupted power supply and voltage stability. Together, they enable efficient energy utilization, continuous operation, and extended system lifespan, making the system effective in both grid-connected and off-grid settings.

Central to the operation of the system is the VCR cycle, comprising a compressor, condenser, expansion valve, and evaporator. The compressor plays a crucial role in compressing the refrigerant vapor, raising its pressure and temperature. The high-pressure, high-temperature vapor then flows to the condenser (2), where it releases heat to the surroundings and condenses into a liquid. This liquid refrigerant (3) passes through the expansion valve, which reduces its pressure and temperature before

entering the evaporator. In the evaporator, the refrigerant (4) absorbs heat from the cooling space, causing it to evaporate and provide cooling. The vaporized refrigerant (1) is then drawn back into the compressor to repeat the cycle (Fig. 2).

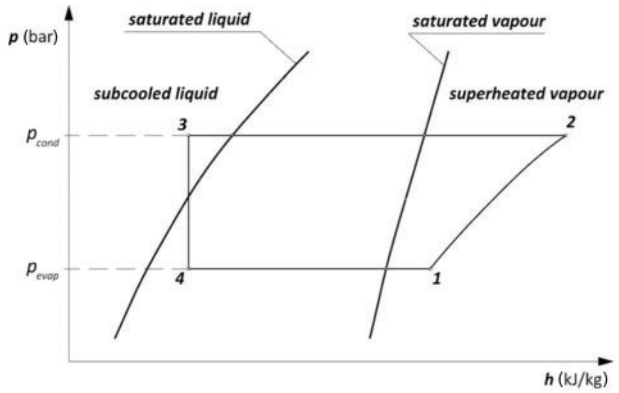


**Figure 2:** Pressure-enthalpy diagram of a vapor compression refrigeration cycle

### *2.2 Site Description*

Ghardaia is located in the M'zab Valley, an oasis region nestled within the northern Sahara Desert of Algeria at 32.26° N latitude and 03.46° E longitude. The climate of Ghardaia is predominantly desertic, with hot, dry summers and mild winters. Average temperatures range from highs of 40°C in summer to lows of 5°C in winter. Despite the searing temperatures, evenings provide little respite, with nighttime lows rarely dropping below 25°C, contributing to the persistent feeling of warmth.

Rainfall in Ghardaia is exceedingly rare, with the city experiencing minimal precipitation throughout the year. The region receives less than 100 millimeters of rainfall annually, most of which occurs sporadically during the winter months. These infrequent showers are often short-lived and provide only temporary relief from the arid conditions. As for solar radiation, the highest monthly value occurs in July as shown in Fig. 3 [17]. Therefore, the month of July has been chosen for the present study as it was found to be the hottest month of the year from the real measured data.

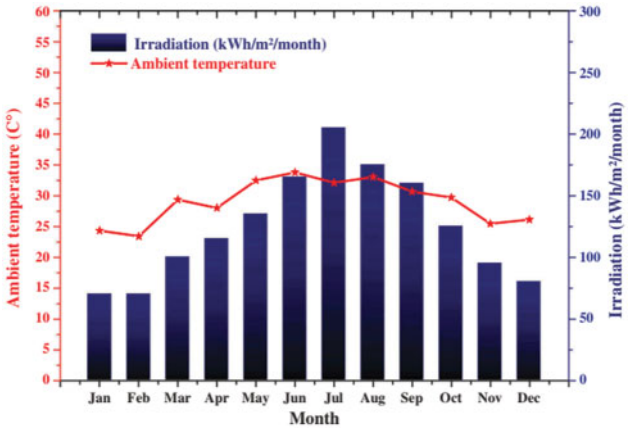


**Figure 3:** Monthly solar irradiation and monthly average daily ambient temperature for the region of Ghardaïa [17]

### *2.3 Working Fluids*

R134a, also identified as 1,1,1,2-Tetrafluoroethane, carries the chemical formula $CH_2FCF_3$ and falls within the HFC family of refrigerants. This colorless, odorless gas exhibits a higher boiling point (–26.3°C) and critical temperature (101°C) in comparison to R1234ze(E), rendering it suitable for medium-temperature refrigeration applications. However, its environmental profile differs from R1234ze(E) due to a relatively high GWP of approximately 1430 over 100 years, contributing significantly to global warming when released into the atmosphere. Despite this, R134a boasts zero ozone depletion potential (ODP). Historically, R134a has found extensive usage as a refrigerant in automotive air conditioning systems, residential and commercial refrigeration, and heat pump applications. Nonetheless, growing environmental concerns and regulatory pressures have prompted a transition towards more sustainable alternatives such as R1234ze(E), advocating for reduced environmental impact in cooling technologies [18].

R1234ze(E) is an HFO refrigerant with the chemical formula CH2=CFCF3. As a member of the HFO family, R1234ze(E) is engineered to possess a low GWP and ODP, rendering it environmentally benign. This colorless gas exhibits a slightly sweet odor and boasts a low boiling point of –19.4°C, coupled with a moderate critical temperature of 93.3°C, rendering it suitable for diverse refrigeration and air conditioning applications. Of notable environmental significance is its remarkably low GWP, estimated to be less than 1, a stark contrast to conventional HFC refrigerants like R134a. Consequently, R1234ze(E) makes negligible contributions to global warming and ozone depletion, positioning it as a favorable alternative in mitigating environmental impact. Its applications span commercial and industrial refrigeration systems, air conditioning units, heat pumps, and chillers, driving its adoption in various sectors seeking sustainable refrigeration solutions [19].

The main thermophysical properties of R134a and R1234ze(E) refrigerants are presented in Table A1 [20].

## 3 Exergy Analysis

The detailed energy analysis of the studied SP-VCR system has been performed in previous work by Selloum et al. [21] using the following assumptions:

- Steady-state operation
- Reversible heat transfer
- Polytropic compression
- Negligible variations in kinetic and potential energy
- Insignificant pressure drops
- Constant cooling capacity

The key operational parameters, that govern the SP-VCR cycle's performance are given in Table A2.

Exergy analysis utilizes principles from the first and second laws of thermodynamics. It identifies losses within both the entire system and its components, offering insights into potential thermodynamic enhancements [22]. The specific exergy flow can be precisely defined as:

$$ex = [(h - h_0) - T_0 (s - s_0)] \tag{1}$$

where $h_0$ and $s_0$ are the specific enthalpy and entropy of the fluid, respectively at the environmental conditions $T_0$ and $P_0$.

The total exergy balance, presented in a rate form, is described as [23]:

$$\sum_{in}\left(1-\frac{T_0}{T_i}\right)\dot{Q}_i+\dot{W}_{in}+\sum_{in}\dot{m}_i ex_i=\sum_{out}\left(1-\frac{T_0}{T_i}\right)\dot{Q}_i+\dot{W}_{out}+\sum_{out}\dot{m}_i ex_i+\dot{E}x_D \tag{2}$$

Exergy efficiency serves as a critical metric for assessing the thermodynamic effectiveness of a system or its components. Generally, exergetic efficiency is defined as [24]:

$$\eta_{ex}=\frac{\sum\dot{E}x_{out}}{\sum\dot{E}x_{in}}=1-\frac{\sum\dot{E}x_D}{\sum\dot{E}x_{in}} \tag{3}$$

where: $\sum\dot{E}x_{out}$, $\sum\dot{E}x_{in}$ and $\sum\dot{E}x_D$ are the total exergy recovered, supplied, and destructed, respectively.

### *3.1 Exergy Analysis of the VCR System*

The exergy of the refrigerant circulating within a refrigeration system is defined as follows [25]:

$$\dot{E}x=\dot{m}_r[(h-h_0)-T_0\,(s-s_0)] \tag{4}$$

Exergy destruction, also known as internal exergy destruction losses resulting from system irreversibilities, is determined by the algebraic sum of total exergy at both the inlet and outlet of the system. The general exergy balance equation is given by [26]:

$$\dot{E}x_D=\dot{E}x_{in}-\dot{E}x_{out} \tag{5}$$

The equations describing exergy destruction and exergetic efficiency within each component of the VCR cycle are as follows [27]:

**a) Evaporator:**

$$\left(\dot{E}x_D\right)_{evap}=\dot{E}x_4+\dot{Q}_e\left(1-\left(\frac{T_0}{T_b}\right)\right)-\dot{E}x_1 \tag{6}$$

**b) Compressor:**

$$\left(\dot{E}x_D\right)_{comp}=\dot{E}x_1+\dot{W}_{comp}-\dot{E}x_2 \tag{7}$$

**c) Condenser:**

$$\left(\dot{E}x_D\right)_{cond}=\dot{E}x_2-\dot{E}x_3 \tag{8}$$

**d) Expansion valve:**

$$\left(\dot{E}x_D\right)_{exp}=\dot{E}x_3-\dot{E}x_4 \tag{9}$$

The overall exergy destruction within the system results from the combined exergy destruction occurring in each of its components. The total exergy destruction in the VCR cycle is expressed as follows:

$$\sum\left(\dot{E}x_D\right)=\left(\dot{E}x_D\right)_{evap}+\left(\dot{E}x_D\right)_{comp}+\left(\dot{E}x_D\right)_{cond}+\left(\dot{E}x_D\right)_{exp} \tag{10}$$

For a VCR system, the exergy efficiency is determined by the ratio of the exergy absorbed in the evaporator from the cooled space at the temperature $T_b$ to the actual compressor work input ($\dot{W}_{comp}$) [28]:

$$\eta_{ex} = \frac{\left|\dot{Q}_e\left(1 - \frac{T_0}{T_b}\right)\right|}{\dot{W}_{comp}} \tag{11}$$

### *3.2 Exergy Analysis of Photovoltaic Panels*

The comprehensive expression of the exergy equation for an open system assuming steady-state conditions, derived from the first law of thermodynamics, can be formulated as [29]:

$$\dot{E}x_{in} = \dot{E}x_{out} - \dot{E}x_{loss} \tag{12}$$

The efficiency of energy conversion in the solar PV system is determined using the following equation [30]:

$$\eta_{energy} = \frac{V_{oc} \times I_{sc} \times FF}{A \times G} \tag{13}$$

The maximum power output of the solar PV is given by:

$$P_{max} = V_{oc} \times I_{sc} \times FF = V_{mp} \times I_{mp} \tag{14}$$

The exergy efficiency of the PV module is defined as the proportion of the exergy obtained from the solar PV (exergy output) to the exergy of the solar radiation (exergy input) [31]:

$$\eta_{ex} = \frac{\dot{E}x_{out}}{\dot{E}x_{in}} \tag{15}$$

The input exergy of a photovoltaic (PV) system comprises solely the exergy derived from solar radiation intensity [31,32]:

$$\dot{E}x_{in} = A.G\left[1 - \frac{4}{3}\left(\frac{T_a}{T_s}\right) + \frac{1}{3}\left(\frac{T_a}{T_s}\right)^4\right] \tag{16}$$

The exergy generated by the PV system can be determined by considering the outlet exergy, which encompasses both thermal and electrical exergies [33]:

$$\dot{E}x_{out} = \dot{E}x_{thermal} - \dot{E}x_{electrical} \tag{17}$$

The exergy associated with thermal energy is given by:

$$\dot{E}x_{thermal} = \dot{Q}\left(1 - \frac{T_a}{T_m}\right) \tag{18}$$

where:

$$\dot{Q} = UA\,(T_m - T_a) \tag{19}$$

The total heat loss coefficient of a PV module includes losses from both convection and radiation:

$$U = h_{conv} + h_{rad} \tag{20}$$

The convective heat transfer coefficient is defined as [34]:

$$h_{conv} = 2.8 + 3V_w \tag{21}$$

The radiative heat transfer coefficient between the PV array and its surroundings [34]:

$$h_{rad} = \varepsilon\sigma \left(T_{sky} + T_m\right)\left(T_{sky}^2 + T_m^2\right) \tag{22}$$

The effective sky temperature is calculated as [34]:

$$T_{sky} = T_a + 6 \tag{23}$$

The PV module's temperature can be determined based on the NOCT (Nominal Operating Cell Temperature) value [35]:

$$T_m = T_a + (\text{NOCT} - 20)\,\frac{G}{800} \tag{24}$$

The electrical exergy contained within the generated electrical power of the PV module is expressed as [36,37]:

$$\dot{E}x_{electrial} = V_{oc} \times I_{sc} \times FF \tag{25}$$

The solar PV module technical specifications are given in Table A3.

The governing equations have been implemented and solved in the MATLAB environment. The framework of the numerical model was validated in a previous work [21] against experimental data. The procedure (algorithm) used for the calculations follows the flow chart in Fig. 4.

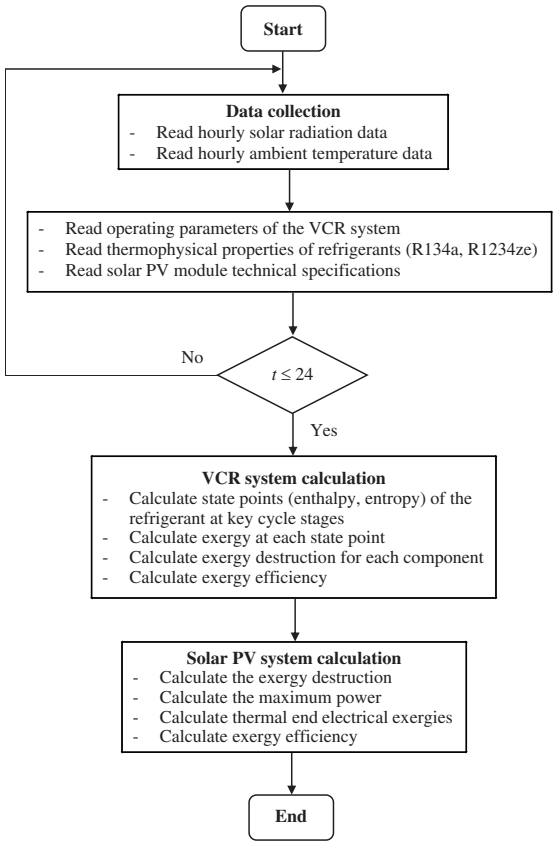


**Figure 4:** The procedure (algorithm) used for the SP-VCR system calculation

## 4 Results and Discussion

### *4.1 Exergy Analysis of the PV System*

The climatic data used in this study (ambient temperature and solar radiation) were measured at the meteorological station situated in the Renewable Energy Applied Research Unit (URAER), Ghardaia. Fig. 5 depicts the input exergy and electrical exergy of the PV module on 21 July. It is obvious from this figure that the electrical exergy generated by the PV module is significantly lower than what could potentially be obtained, primarily due to substantial exergy loss resulting from the irreversibility of the SP-VCR system, such as thermal losses, optical losses, and non-ideal behavior of PV materials. The input exergy pattern closely tracks the global irradiance, with larger differences observed at higher irradiance levels. This signifies that the solar exergy, driven by the sun's high temperature, holds significant potential for performing useful work. it can be also observed that solar irradiation and exergy input rise as sunlight intensifies, peaking around noon. Following this peak, they gradually decline as evening approaches, with minimal to no solar energy influence between 8:00 PM and 4:00 AM.

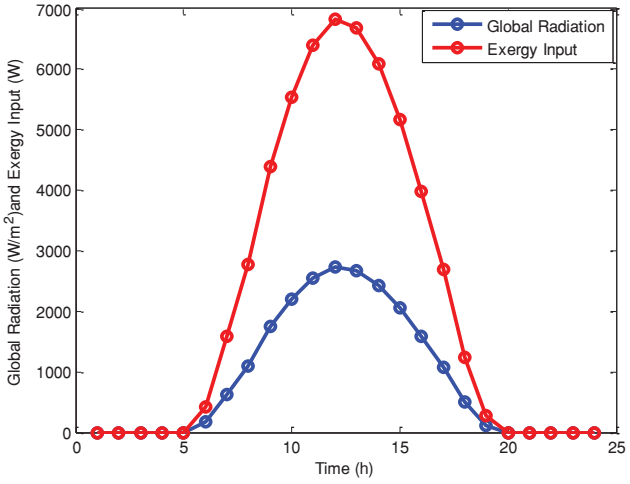


**Figure 5:** Hourly variation of solar radiation intensity and input exergy

Fig. 6 illustrates the fluctuation of exergy efficiency and input exergy on the PV module. The exergy efficiency of the PV system remains relatively modest, reaching its highest point at noon with a value of 33.05%, considerably lower than the theoretically ideal 100% reversible process. This inefficiency is attributed to the irreversible nature of the PV conversion process, leading to a notable dissipation of incident solar exergy on the module. Despite the widespread use and advantages of conventionally available silicon modules, like mono-crystalline silicon, they still incur substantial exergy losses. Notably, mono-crystalline silicon cells, employed in this study, offer the highest efficiency among the three most common crystalline silicon cell technologies, reaching up to 20%. Additionally, it is observed that the exergy efficiency of the PV module rises as solar intensity increases.

Fig. 7 displays the distribution of exergy loss, electrical exergy, exergy input, and thermal exergy on 21 July. As shown in this figure, the trend of the loss exergy variation follows that of the input exergy, and the relative loss of exergy exceeds 66% at noon. This substantial loss highlights the inefficiency in harnessing the high exergy content of sunlight by current silicon modules. The exergy efficiency of conventional silicon solar PV panels is notably low due to the low quality of the output energy, leading to significant exergy losses within the panels. The maximum values of electrical exergy and thermal

exergy of the SP-VCR system are 9145 and 7506 W, respectively. The electric efficiency is higher than thermal efficiency, which means that most of the heat has been wasted and absorbed by the solar panel.

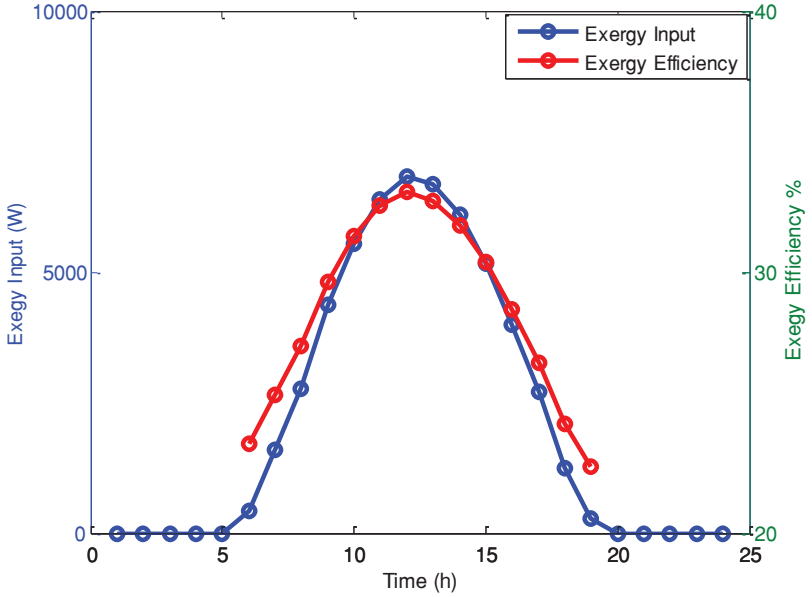


**Figure 6:** Hourly variation of input solar exergy and exergy efficiency

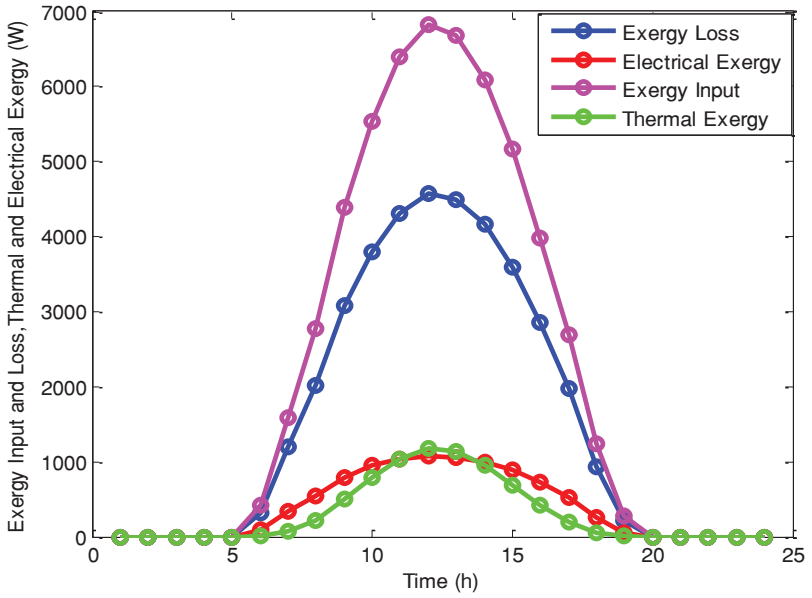


**Figure 7:** Hourly variation of exergy loss, electrical exergy, exergy input, and thermal exergy

Fig. 8 shows the hourly changes in energy and exergy efficiencies of the SP-VCR system. It can be seen that the maximum energy and exergy efficiency values at noon are 21.12% and 33.05%, respectively. As temperature increases, the exergy efficiency increases while the energy efficiency drops due to heat losses from the system. The results agree with the findings of Oruc et al. [38]. It can also

be seen that the exergy efficiency is much higher than the energy efficiency because of the substantial degradation of energy quality imposed by the second law of thermodynamics. To achieve optimal energy and exergy efficiencies, it is imperative to maintain the temperature of the PV module close to its operating temperature, which essentially means controlling the PV module temperature through surface cooling using either water or air.

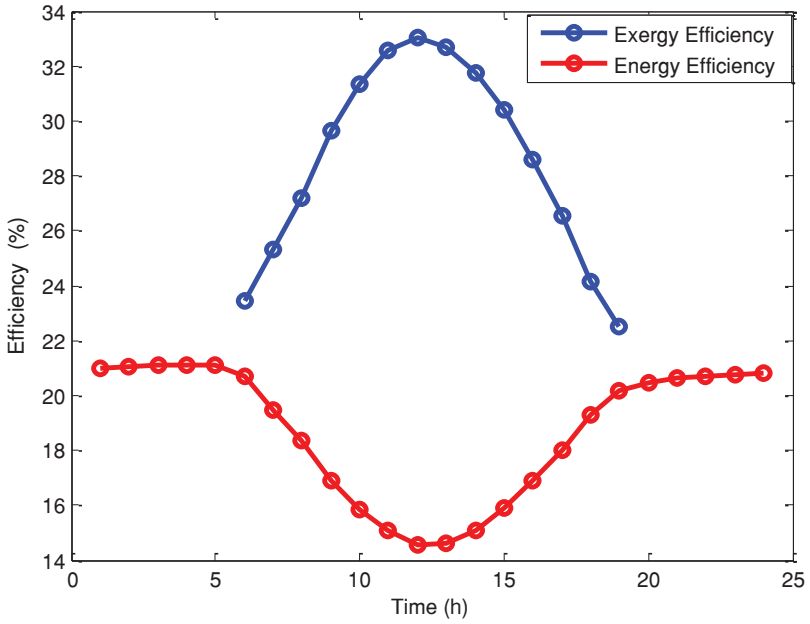


**Figure 8:** Hourly variation of energy and exergy efficiencies

### *4.2 Exergy Analysis of the VCR System*

Fig. 9 illustrates how the exergy efficiency of the VCR system is influenced by ambient temperature for both refrigerants R134a and R1234ze(E). The exergy efficiency increases as ambient temperature rises due to the increased compressor work. However, R1234ze(E) exhibits higher exergy efficiency compared to R134a with maximum values of 28.06% and 14.95%, respectively. The lower irreversibility observed when using R1234ze(E) compared to R134a can be attributed to several factors. First, R1234ze(E) exhibits more favorable thermodynamic properties such as lower pressure ratios and higher volumetric efficiencies, which result in reduced thermodynamic losses during compression and expansion processes. In addition, R1234ze(E) demonstrates superior heat transfer performance, particularly at higher temperatures, leading to more efficient heat exchange in the evaporator and condenser and minimizing irreversibility associated with heat transfer processes. These results are in agreement with previous findings from other studies [8,27].

Fig. 10 illustrates the changes in exergy efficiency with evaporating temperature for both R134a and R1234ze(E) refrigerants in the VCR cycle. As the evaporating temperature increases, the exergy efficiency decreases due to the decrease of the compressor work and the increase of heat transfer in the evaporator. The trend is the same for both refrigerants. However, the irreversibilities within the R1234ze(E) cycle are notably lower compared to that of R134a, as shown in Fig. 11. The average second-law efficiency increase is about 45% when using R1234ze(E) in the VCR cycle. The average exergy destruction for R1234ze(E) is around 55% smaller than R134a.

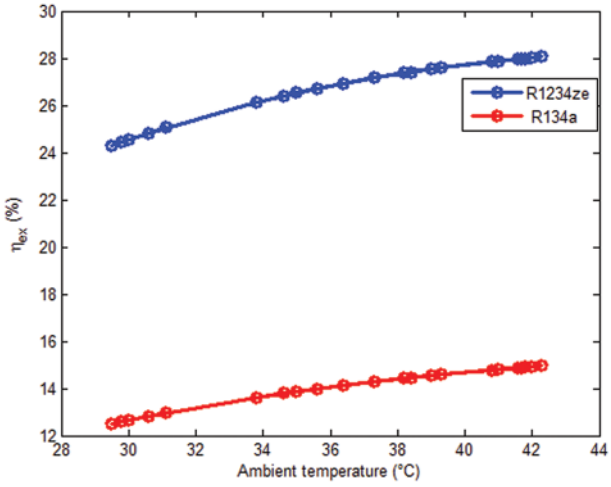


**Figure 9:** Variation of exergy efficiency of the VCR cycle with ambient temperature ($T_{ev} = 0°C$)

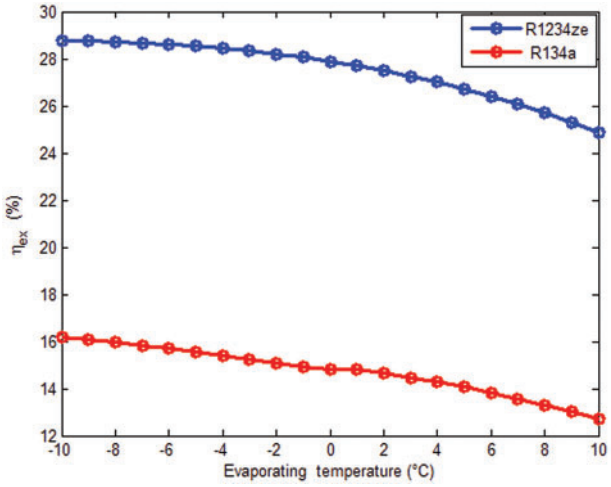


**Figure 10:** Variation of exergy efficiency of the VCR cycle with evaporating temperature

The exergy destructions of the main components of the VCR system are compared in Fig. 12 for $T_{ev} = 0°C$ at noon on July 21 using both studied refrigerants. It can be seen that the compressor exhibits the highest exergy destruction, followed by the condenser, expansion valve, and evaporator. For R1234ze(E) fluid, the total irreversibility is 0.57 kW, distributed as follows: compressor 40.71%, condenser 25.77%, expansion valve 20.07%, and evaporator 13.45%. On the other hand, the total irreversibility for R134a refrigerant is 0.82 kW, with 65.09% occurring in the compressor, 18.04% in the condenser, 10.50% in the expansion valve, and 6.37% in the evaporator.

Therefore, improving the compressor's efficiency will have the most significant impact on reducing overall system irreversibility and enhancing exergy efficiency. This can be achieved by implementing advanced designs like variable-speed or multi-stage compressors, using materials with superior thermal properties and durability, optimizing lubrication systems to reduce friction losses, maintaining a rigorous maintenance schedule to ensure peak performance, and integrating heat recovery systems to

utilize waste heat. These measures will collectively reduce energy losses and improve the compressor's efficiency, leading to a more efficient and effective overall system.

Fig. 13 depicts the comparative irreversibility of individual components when utilizing R134a and R1234ze(E), respectively. Across all components and the whole system, R1234ze(E) exhibits lower irreversibility compared to R134a. Specifically, the improvements made with R1234ze(E) are 71.95% for the compressor, 39.13% for the condenser, 15.38% for the expansion valve, 5% for the evaporator, and 54.76% for the overall system.

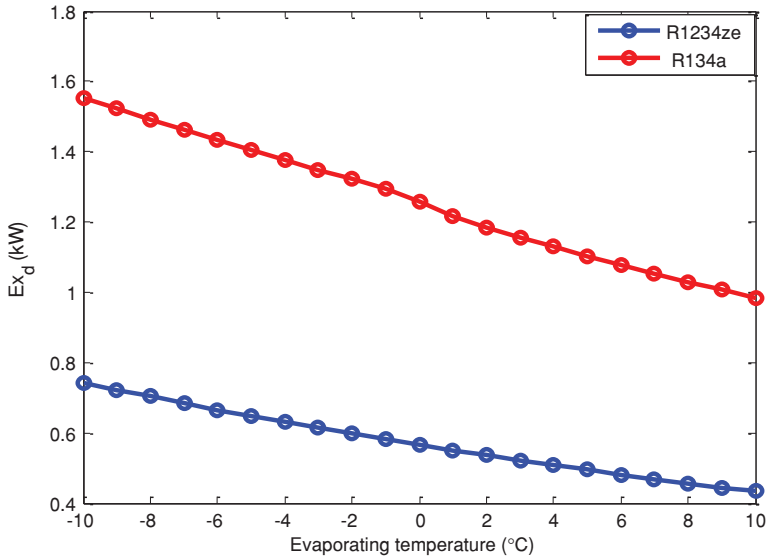


**Figure 11:** Variation of total exergy destruction of the VCR cycle with evaporating temperature

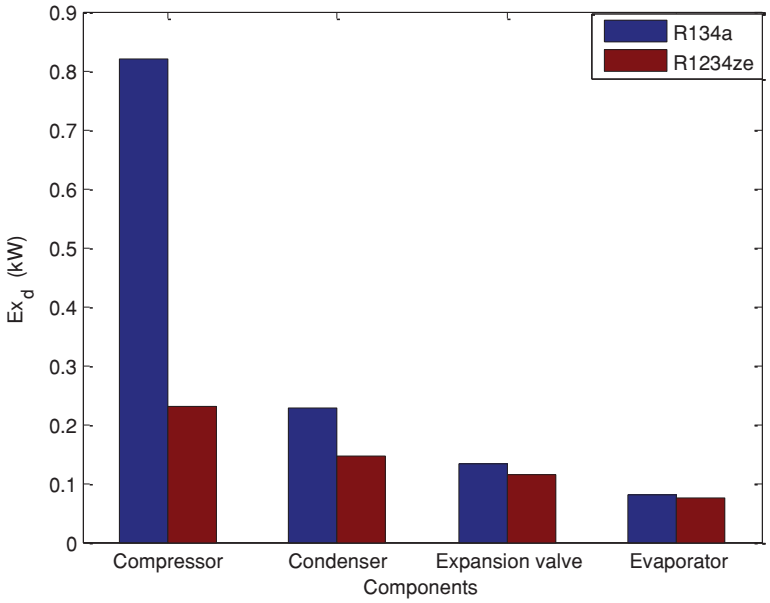


**Figure 12:** Exergy destruction in each component of the VCR cycle

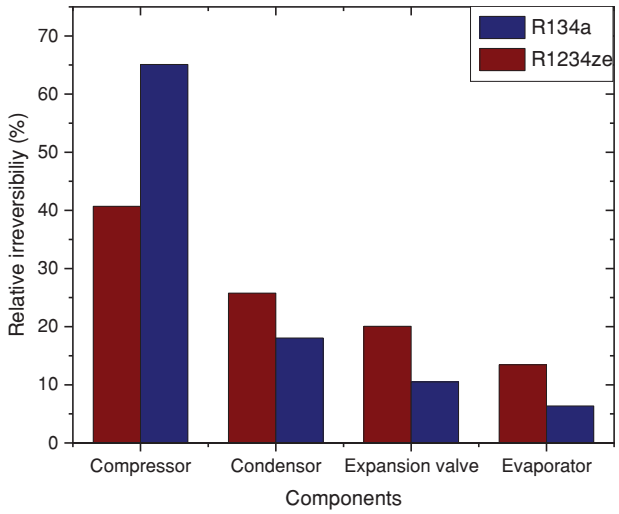


**Figure 13:** Relatives irreversibilities for different components

### *4.3 Industrial Implication*

The findings of this study have significant industrial implications, particularly for sectors reliant on refrigeration systems, such as food storage, pharmaceuticals, and chemical processing. The demonstrated exergy efficiency improvements with R1234ze(E) as a replacement for R134a highlight several key advantages for industrial applications. Firstly, the substantial improvements in exergy efficiency, especially the 71.95% enhancement in compressor performance, indicate a considerable reduction in energy consumption. This can lead to lower operational costs for industries, which is crucial given the high energy demand for refrigeration systems. Reduced energy consumption translates directly into cost savings, making operations more economically viable.

Moreover, the adoption of R1234ze(E) aligns with global efforts to reduce greenhouse gas emissions and combat climate change. By demonstrating lower irreversibility and improved overall system efficiency, this study supports the transition to eco-friendly refrigerants. This shift can help industries meet environmental regulations and sustainability goals, thus reducing their carbon footprint and contributing to global environmental conservation efforts.

Additionally, the enhanced efficiency and reduced exergy destruction across system components (compressor, condenser, expansion valve, and evaporator) suggest that systems using R1234ze(E) may experience less wear and tear. This can lead to extended equipment lifespan, reduced maintenance needs, and lower replacement costs, which are significant considerations for industrial operations. Longer-lasting equipment and less frequent maintenance can improve operational reliability and reduce downtime.

Furthermore, with increasing regulatory pressures to phase out high-GWP (Global Warming Potential) refrigerants like R134a, the industrial adoption of R1234ze(E) can facilitate compliance with environmental standards and avoid potential penalties. The demonstrated performance benefits provide a strong case for industries to invest in retrofitting or upgrading their existing systems, ensuring they stay ahead of regulatory changes and avoid costly fines.

Also, industries that adopt advanced, eco-friendly refrigeration technologies can enhance their market competitiveness by promoting their commitment to sustainability and energy efficiency. This

can be a significant differentiator in markets where consumers and stakeholders increasingly value environmental responsibility. Companies can leverage their green credentials to attract environmentally conscious customers and investors.

Finally, the study's methodology and findings can spur further research and innovation in the development of next-generation refrigeration systems. Industries can leverage these insights to explore new designs, materials, and technologies that further enhance efficiency and sustainability. Continuous innovation can lead to the development of even more advanced refrigeration systems, driving progress in industrial cooling applications.

## 5 Conclusion

In this paper, exergy analysis was conducted on a SP-VCR system situated in the Ghardaïa region of southern Algeria using MATLAB software programming. In addition, a performance comparison has been performed between two working refrigerants: R134a and its potential alternative, R1234ze(E). The following are the conclusions drawn from the present study:

- Environmental conditions have significant effects on exergy loss, electrical exergy, exergy input, and thermal exergy of the SP-VCR system.
- The maximum values of electrical exergy and thermal exergy of the SP-VCR system are 9145 and 7506 W, respectively.
- The exergy efficiency of the PV modules is very low (33.05%) indicating that current silicon modules use only a small portion of the considerable exergy content present in solar radiation.
- The maximum energy and exergy efficiency values at noon are 21.12% and 33.05%, respectively.
- The exergy efficiency of the SP-VCR system increases with rising ambient temperature and is notably higher with R1234ze(E) compared to R134a.
- The exergy efficiency of the refrigeration system decreases as the evaporating temperature rises, with R1234ze(E) displaying superior performance over R134a.
- Exergy destruction is primarily attributed to the compressor, followed by the condenser, expansion valve, and evaporator.
- R1234ze(E) refrigerant exhibits higher exergy efficiency compared to R134a with maximum values of 28.06% and 14.95%, respectively.

Finally, despite its modest exergy efficiency and notable exergy destruction, a SP-VCR system using low GWP refrigerants remains a promising environmentally friendly solution, especially for remote locations with ample solar radiation. Furthermore, Enhancements in system design and component characteristics are pivotal for minimizing irreversibilities, particularly within the solar PV panels, which contribute significantly to overall system irreversibilities. Therefore, it is crucial to maintain the PV module temperature close to its operational level to optimize the exergy efficiency of the entire system.

**Acknowledgement:** This work was supported in the entire part by the Biomaterials and Transport Phenomena Laboratory Agreement No. 303 03-12-2003, at the University of Medea. The authors acknowledge and gratefully thank the financial support provided by DG-RSDT of Algeria.

**Funding Statement:** The authors received no specific funding for this study.

**Author Contributions:** The authors confirm their contribution to the paper as follows: study conception and design: Zakaria Triki, Ahmed Selloum, Younes Chiba; data collection: Zakaria Triki, Ahmed Selloum; analysis and interpretation of results: Zakaria Triki, Ahmed Selloum, Younes Chiba; draft manuscript preparation: Hichem Tahraoui, Dorsaf Mansour, Abdeltif Amrane, Meriem Zamouche, Mohammed Kebir, Jie Zhang. All authors reviewed the results and approved the final version of the manuscript.

**Availability of Data and Materials:** Not applicable.

**Conflicts of Interest:** The authors declare that they have no conflicts of interest to report regarding the present study.

## References


1. Aung, M. M., Chang, Y. S. (2022). *Cold chain management; springer series in advanced manufacturing*. Berlin: Springer International Publishing. https://doi.org/10.1007/978-3-031-09567-2
2. Dong, Y., Coleman, M., Miller, S. A. (2021). Greenhouse gas emissions from air conditioning and refrigeration service expansion in developing countries. *Annual Review of Environment and Resources, 46,* 59–83. https://doi.org/10.1146/annurev-environ-012220-034103
3. Moran, M. J., Sciubba, E. (1994). Exergy analysis: Principles and practice. *ASME Journal of Engineering for Gas Turbines and Power, 116(2),* 285–290. https://doi.org/10.1115/1.2906818
4. Bibin, B. S., Gundabattini, E. (2021). Properties and performance of eco-friendly hydro-fluoro-olefin (HFO) refrigerant-R1234yf: Part I. *International Journal of Air-Conditioning and Refrigeration, 29(3),* 2130005. https://doi.org/10.1142/S2010132521300056
5. Yumrutaş, R., Kunduz, M., Kanoğlu, M. (2002). Exergy analysis of vapor compression refrigeration systems. *Exergy, An International Journal, 2,* 266–272. https://doi.org/10.1016/S1164-0235(02)00079-1
6. Rashid, F. L., Eleiwi, M. A., Mohammed, H. I., Ameen, A., Ahmad, S. (2023). A review of using solar energy for cooling systems: Applications, challenges, and effects. *Energies, 16(24),* 8075. https://doi.org/10.3390/en16248075
7. Sudhakar, K., Srivastava, T. (2014). Energy and exergy analysis of 36 W solar photovoltaic module. *International Journal of Ambient Energy, 35,* 51–57. https://doi.org/10.1080/01430750.2013.770799
8. Jemaa, R. B., Mansouri, R., Boukholda, I., Bellagi, A. (2017). Energy and exergy investigation of R1234ze(E) as R134a replacement in vapor compression chillers. *International Journal of Hydrogen Energy, 42,* 12877–12887.
9. Dhondge, A., Kalbande, S. (2019). Energy and exergy analysis of SPV powered vapor compression refrigeration system. *Multilogic in Science, 8,* 181–183.
10. Haiyan, L., Wei, G., Chuanshan, D. (2019). Experimental study of a micro-refrigeration system driven by photovoltaic power generation. *Energy Procedia, 158,* 516–521. https://doi.org/10.1016/j.egypro.2019.01.145
11. Omer, D. A., Mahdi, M., Shuraiji, A. L. (2021). An experimental study optimization of a solar assisted D.C Refiergerter under Iraqi climate. *Journal of Physics: Conference Series, 1973(1),* 012082. https://doi.org/10.1088/1742-6596/1973/1/012082
12. Amaris, C., Barbosa, F., Balbis, M. (2023). Energy performance analysis of a solar refrigerator using ecological refrigerants. *Journal of Sustainable Development of Energy Water and Environment Systems, 11(2),* 1–25. https://doi.org/10.13044/j.sdewes.d11.0446
13. Khan, Y., Faruque, M. W., Nabil, M. H., Ehsan, M. M. (2023). Ejector, and vapor injection enhanced novel compression-absorption cascade refrigeration systems: A thermodynamic parametric

and refrigerant analysis. *Energy Conversion and Management, 289(5822),* 117190. https://doi.org/10.1016/j.enconman.2023.117190

14. Nabil, M. H., Khan, Y., Faruque, M. W., Ehsan, M. M. (2023). Thermo-economic assessment of advanced triple cascade refrigeration system incorporating a flash tank and suction line heat exchanger. *Energy Conversion and Management, 295(7),* 117630. https://doi.org/10.1016/j.enconman.2023.117630
15. Albà, C. G., Alkhatib, I. I., Lovell, F., Vega, L. F. (2024). A novel approach for designing efficient and sustainable cooling cycles with low global warming refrigerants. *Applied Thermal Engineering, 246(B),* 122895. https://doi.org/10.1016/j.applthermaleng.2024.122895
16. Al-Rbaihat, R., Alahmer, H., Al-Manea, A., Altork, Y., Alrbai, M. et al. (2024). Maximizing efficiency in solar ammonia-water absorption refrigeration cycles: Exergy analysis, concentration impact, and advanced optimization with GBRT machine learning and FHO optimizer. *International Journal of Refrigeration, 161,* 31–50. https://doi.org/10.1016/j.ijrefrig.2024.01.028
17. Zaghba, L., Khennane, M., Fezzani, A., Borni, A., Hadj Mahammed, I. (2021). Experimental performance assessment of a 2.25 kWp Rooftop PV system installed in the desert environment: A case study of Ghardaia. *Algeria International Journal of Sustainable Engineering, 14(3),* 517–528.
18. Hodnebrog, Ø., Etminan, M., Fuglestvedt, J. S., Marston, G., Myhre, G. et al. (2013). Global warming potentials and radiative efficiencies of halocarbons and related compounds: A comprehensive review. *Reviews of Geophysics, 51(2),* 300–378.
19. Censi, G., Padovan, A. (2021). R1234ze(E) as drop-in replacement for R134a in a micro-fin shell-and-tube evaporator: Experimental tests and calculation model evaporator: Experimental tests and calculation model. *Proceedings of the 18th International Refrigeration and Air Conditioning Conference*, West Lafayette, IN, USA.
20. Mota-Babiloni, A., Navarro-Esbrí, J., Mendoza-Miranda, J. M., Peris, B. (2017). Experimental evaluation of system modifications to increase R1234ze(E) cooling capacity. *Applied Thermal Engineering, 111,* 786–792.
21. Selloum, A., Triki, Z., Chiba, Y. (2024). Thermodynamic analysis of a solar-driven vapor compression refrigeration system using R1234ze(E) for cooling applications in Ghardaïa region (Southern Algeria). *Journal of Thermal Engineering, 10(1),* 130–141.
22. Dincer, I., Rosen, MA. (2013). *Exergy, energy, and environment sustainable development*, 2nd edition. Oxford, UK: Elsevier Ltd. Publication.
23. Bouaziz, N., Lounissi, D. (2015). Energy and exergy investigation of a novel double effect hybrid absorption refrigeration system for solar cooling. *International Journal of Hydrogen Energy, 40(39),* 13849e56.
24. Terzi, R., Tükenmez, I., Kurt, E. (2016). Energy and exergy analyses of a_VVER type nuclear power plant. *International Journal of Hydrogen Energy, 41(29),* 12465e76.
25. Bejan, A. B. A., Tsatsaroni, G., Moran, M. (1996). *Thermal design & optimization*. New York: John Wiley & Sons Inc.
26. Dincer, I., Kanoglu, M. (2010). *Refrigeration systems, and applications*. New York: Wiley.
27. Agarwal, S., Arora, A., Arora, B. B. (2021). Energy and exergy investigations of R1234yf and R1234ze as R134a replacements in mechanically subcooled vapour compression refrigeration cycle. *Journal of Thermal Engineering, 7(1),* 109–132.
28. Arora, A., Kaushik, SC. (2008). Theoretical analysis of a vapour compression refrigeration system with R502, R404A, and R507A. *International Journal of Refrigeration, 31(6),* 998–1005. https://doi.org/10.1016/j.ijrefrig.2007.12.015
29. Wong, K. F. V. (2000). *Thermodynamics for engineers*. Boca Raton, FL, USA: University of Miami, CRC Press LLC.
30. Sahin, A. D., Dincer, I., Rosen, M. A. (2007). Thermodynamic analysis of solar photovoltaic cell systems. *Solar Energy Materials & Solar Cells, 91,* 153–159.

31. Petela, R. (2003). Exergy of undiluted thermal radiation. *Solar Energy, 74,* 469–488. https://doi.org/10.1016/S0038-092X(03)00226-3
32. Petela, R. (2008). An approach to the exergy analysis of photosynthesis. *Solar Energy, 82(3),* 11–328. https://doi.org/10.1016/j.solener.2007.09.002
33. Sarhaddi, F., Farahat, S., Ajam, H., Behzadmehr, A. (2010). Exergetic performance evaluation of a solar photovoltaic (PV) array. *Australian Journal of Basic and Applied Sciences, 4(3),* 502–519.
34. Watmuff, J. H., Charters, W. W. S., Proctor, D. (1977). *Solar and wind-induced external coefficients for solar collectors*. Cooperation Mediterraneenne pour l'Energie Solaire.
35. Ross Jr, R. (1980). Flat-plate photovoltaic array design optimization. *14th Photovoltaic Specialists Conference*, pp. 1126–1132. San Diego, CA, USA.
36. Joshi, A. S., Tiwari, A. (2007). Energy and exergy efficiencies of a hybrid photovoltaic-thermal (PV/T) air collector. *Renewable Energy, 32(13),* 2223–2241. https://doi.org/10.1016/j.renene.2006.11.013
37. Joshi, A. S., Dincer, I., Reddy, B. V. (2009b). Thermodynamic assessment of photovoltaic systems. *Solar Energy, 83(8),* 1139–1149. https://doi.org/10.1016/j.solener.2009.01.011
38. Oruc, M. E., Desai, A. V., Kenis, P. J. A., Nuzzo, R. G. (2016). Comprehensive energy analysis of a photovoltaic thermal water electrolyzer. *Applied Energy, 164,* 294–302. https://doi.org/10.1016/j.apenergy.2015.11.078

## Appendix A

**Table A1:** Refrigerant properties of R134a and R1234ze(E)

| Property | R134a | R1234ze(E) |
|---|---|---|
| ASHRAE safety classification | A1 | A2L |
| ODP (Ozone depletion potential) | 0 | 0 |
| GWP (Global warming potential) | 1430 | 7 |
| Critical temperature (K) | 247.08 | 253.88 |
| Critical pressure (kPa) | 4059.28 | 3623.90 |
| Specific heat ratio ($\gamma$) | 1.12 | 1.101 |
| Vapor density (kg·m$^{-3}$) | 14.35 | 11.65 |
| Liquid density (kg·m$^{-3}$) | 1295 | 1240 |
| Latent heat of vaporization (kJ·kg$^{-1}$) | 198.72 | 184.28 |

**Table A2:** Operating parameters of the VCR system

| Parameter | Value |
|---|---|
| Nominal cooling capacity | 2 kW |
| Evaporating Temperature | 0°C |
| Condenser temperature approach | 15 K |
| Superheat | 5 K |
| Subcooling | 5 K |
| Electric motor efficiency | 95% |
| Belt transmission efficiency | 100% (direct transmission) |
| Compressor mechanic efficiency | 80% |
| Polytropic efficiency | 75% |

**Table A3:** Solar PV module technical specifications

| Parameter | Value |
|---|---|
| PV panel efficiency | 21.5% |
| Peak power of the unit photovoltaic field | 580 W |
| NOCT | 43°C |
| PV panel emissivity | 0.9 |
| Open circuit voltage ($V_{oc}$) | 46.3 V |
| Short circuit current ($I_{sc}$) | 15.94 A |
| Number of photovoltaic cells | 132 |
| Maximum circuit voltage ($V_{mp}$) | 39 V |
| Maximum circuit current ($I_{mp}$) | 14.86 A |
| Dimensions | 2384 mm × 1134 mm × 35 mm |
| Weight | 29.1 kg |
| Module surface | 2.703456 $m^2$ |
| Fill Factor | 0.7859 |
| Stefan Boltzmann constant ($\sigma$) | $5.67 \times 10^{-8}$ $W/m^2.K^4$ |
| Sun temperature | 5780 K |